ORIGINAL ARTICLE

Hydrogeochemical analysis and assessment of mine water quality in Tangjiahui mining area, Inner Mongolia, China

Shidong Wang[1,2] · Hongwei Tang[1,2] · Lei Shi[1,2] · Ji Liu[1,2] · Zhibin Yang[1,2] · Hongjun Zhu[1,2] · Feng Xu[1,2] · Kaipeng Zhu[1,2] · Juan Fan[1,2] · Gang Fang[1,2]

Abstract

Mine water plays an essential role in securing mine production and domestic consumption in arid mining areas. This study was conducted to analyse the hydrogeochemical characteristics, determine the hydrochemical processes and assess the quality of mine water in the Tangjiahui mining area in Jungar Coalfield, Inner Mongolia, China, by using the Piper trilinear diagram, Gibbs map and statistical methods. The results showed that the pH and EC of the mine water in the study area ranged from 7.10 to 7.90 and from 1684.70 to 3435.60 µS/cm, respectively. The TH and TDS were in the range of 219.52–390.6 mg/L and 926.61 to 1889.56 mg/L, respectively. The cation content in the mine water was ranked from the highest to the lowest as $Na^+ > Ca^{2+} > Mg^{2+}$, while the anion content was ranked as $Cl^- > HCO_3^- > SO_4^{2-}$. The hydrochemical type of the mine water was Cl–Na. The main mechanisms controlling the major chemistry of the mine water were the dissolution of halite and gypsum, and reverse cation exchange. Due to its high concentration of major ions, TDS, EC, SAR, and Na%, the mine water in the study area was not suitable for human consumption and agricultural irrigation. These results are beneficial for the sustainable reuse and management of mine water resources in the mining area, and will also provide references for similar studies in other regions of the world.

Keywords Mine water · Tangjiahui mining area · Hydrochemical characteristics · Piper trilinear diagram · Gibbs map · Ion source

Introduction

Coal mining plays an important role in the economic development of many countries worldwide (Schneider et al. 2012; Li et al. 2015). According to information disclosed by the Energy Information Administration (EIA 2019) of the USA, the total global coal output in 2019 was around 7.6 billion tons, of which China's contribution was around 3.7455 billion tons, or nearly 50% of the total (Yu et al. 2020). Coal accounts for over 60% of China's energy production and consumption, and is therefore the main energy source in the country (Liu et al. 2020). However, within the country, coal and water resources show a reverse distribution—that is, areas with abundant coal resources basically lack in water resources (Wu et al. 2017). For example, the water-scarce arid and semi-arid regions of western China have extremely abundant coal resources. These water shortages are exacerbated by the coal mining process, as in order to prevent flood accident occurrence, a large amount of mine water is required to be drained before or during coal mining (Huang et al. 2017; Xu et al. 2019). Therefore, research on mine water reuse is critical toward finding ways of mitigating this problem. As the quality of the mine water directly affects its usefulness in different applications, the development of quality evaluation protocols is of great importance toward the sustainable utilization of mine water resources in western China (Li 2018; Liu et al. 2020).

The hydrochemical characteristics of groundwater can directly reflect its quality, and possible changes in the groundwater quality can be indirectly understood via

✉ Shidong Wang
  wangshidong@cctegxian.com

✉ Ji Liu
  g73018606@126.com

1   Xi'an Research Institute of China, Coal Technology & Engineering Group Corp, Xi'an 710054, Shaanxi, China

2   Key Laboratory of Coal Mine Water Hazard Prevention and Control Technology in Shaanxi Province, Xi'an 710054, Shaanxi, China

analysis of the factors influencing these characteristics, making this a valuable area of study (Li et al. 2018; Liu et al. 2019a). To date, therefore plenty of research has been carried out on the hydrochemical characteristics of groundwater. The conventional Piper trilinear diagram (Piper 1944) and Gibbs map (Gibbs 1970) have been widely used to determine the hydrochemical characteristics and influencing factors of the groundwater. In recent years, it has been found that a combination of statistical and conventional methods is more effective compared to traditional approaches (Redwan et al. 2016; Wang et al. 2017; Li et al. 2018; Sefie et al. 2018). Li et al. (2013a, b) used a correlation analysis method in conjunction with the Piper trilinear diagram and Gibbs map to determine the hydrochemical characteristics and influencing factors for the shallow groundwater in both Pengyang County and Dongsheng Coalfield in China. Cloutier et al. (2008) used principal component analysis (PCA) and other conventional methods to determine the hydrochemical processes occurring in the groundwater in Basses–Laurentides, Canada.

The Tangjiahui coal mining area is part of the Jungar Coalfield, which is located in the arid and semi-arid regions of Inner Mongolia. The continuation of coal seam mining in Tangjiahui is threatened by the Ordovician limestone karst fissure aquifer, which is the main local water resource, so a large amount of mine water is required to be drained before and during the mining process (Li et al. 2020). If mine water cannot be reused, the valuable water resources are wasted.

Therefore, the main objectives of this study are (1) to analyze the hydrogeochemical characteristics and identify the hydrochemical processes, and (2) to assess the quality of mine water by collecting water samples during the mining process in Tangjiahui mining area. This will provide a scientific basis for local water resource management and rational utilization of mine water in the area.

Overview of the study area

The Tangjiahui coal mining area is located in the central part of the Jungar Coalfield in Ordos City (Fig. 1). The area of the mining field is 28.58 km^2, and the minable coal seams are Nos. 4, 5, 6, 9 upper, and 9 lower, with a resource reserve of 0.805 billion tons. Of these, the main coal seam is No. 6, with a design capacity of 6 million ton/year. The coal mine was constructed in October 2010 and put into operation in 2013. The study area is arid and semi-arid with occasional rain. The average annual precipitation is around 400 mm, and the rainfall is mainly concentrated in the three summer months of July, August, and September, which account for 60–70% of the annual precipitation. The evaporation is intense, with average annual evaporation > 2000 mm, resulting in a relative lack of local groundwater resources.

The surface drainage in the study area is mainly the Yellow River. Riverside source fields (the main water source is the Ordovician aquifer) were constructed in areas where the Yellow River flows through, providing domestic water for residents.

Most of the mining area is covered by Quaternary wind-deposited sand, but there are also bedrock outcrops on both sides of the gully and in the origin of the gully (Fig. 1). The formations are ranked from oldest to newest as follows: Middle Ordovician Majiagou Formation (O_2m), Upper Carboniferous System Taiyuan Formation (C_2t), Lower Permian Shanxi Formation (P_1s), Lower Shihezi Formation (P_1x), Upper Shihezi Formation (P_2s), Shiqianfeng Formation (P_2sh), Lower Cretaceous Zhidan Group (K_1zh), Neogene Pliocene (N_2), and Quaternary System (Q). The maximum thickness of the O_2m stratum is 234 m, formed by light gray thick layered limestone and dolomitic limestone and the thickness of the C_2t, P_1s, P_1x, P_2s and P_2sh stratum is 53.00–109.89 m, 38.42–167.72 m, 61.23–152.80 m, 59.30–199.19 m and 11.35–226.01 m, respectively, consisting of mudstone, sand mudstone and quartz sandstone. Additionally, the K_1zh stratum is composed of light red, brick red gravelly coarse-grained sandstone and glutenite, with a thickness of 20.02–104.02 m and the N_2 stratum is a red and brownish red sandy clay layer with a thickness of less than 15 m. The Q stratum is composed of loess and aeolian sand, with a thickness of less than 100 m. The main coal seam in the study area is located at the Taiyuan Formation stratum, which is mainly threatened by the Ordovician limestone aquifer with high water pressure and abundant water during the seam mining process. The depth of the rock aquifer is more than 500 m, and it contains geological features such as corrosion fissures, karst caves, and dissolved pores. The unit water yield of the Ordovician limestone aquifer is 0.024–34.321 L/s m, and the water abundance varies from weak to very strong. Therefore, to prevent the occurrence of water hazard accidents, the pressure and amount of water in the aquifer should be reduced to safe levels through drilling drainage before mining.

Sample collection and testing

In total, 34 mine water samples were collected from the drainage boreholes in situ during the mining process. For each water sample, 1 L was collected. Prior to sample collection, the container was rinsed with the sampled water three times. After collection, the water sample container was immediately covered, sealed, and labeled with the sample collection time, sampling number, and name of the sample collector.

The test indicators for the water sample include pH, EC, cations ($Na^+ + K^+$, Ca^{2+} and Mg^{2+}), anions (Cl^-, SO_4^{2-} and

Fig. 1 Location of the study area
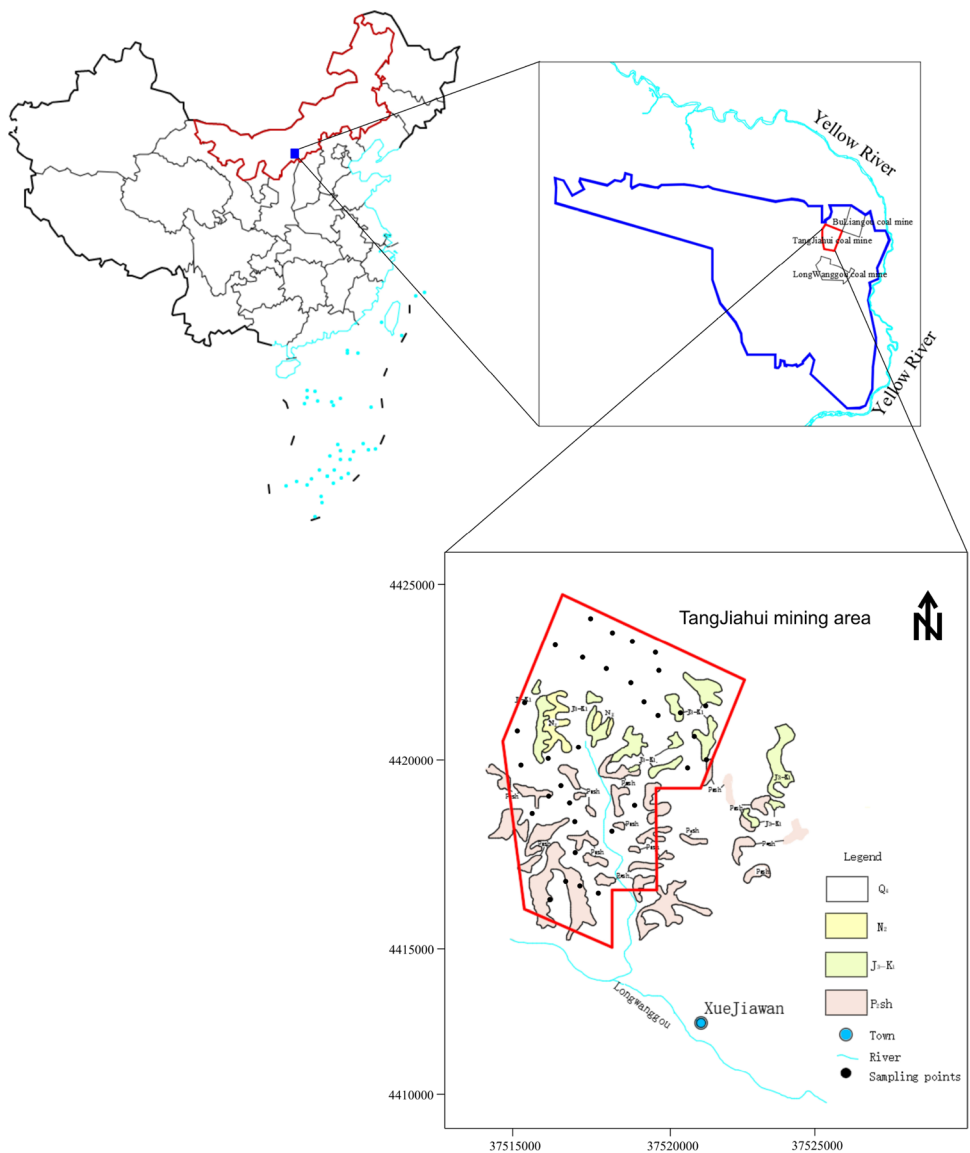
HCO$_3^-$), total hardness (TH), and total dissolved solids (TDS). Of these, pH and EC were measured in situ using the German HI9829 high-precision portable multi-parameter integrated water quality tester. The cations and cation concentrations were determined by plasma spectrometer (IRIS Intrepid II XSP, Thermo Electron, USA) and ion chromatograph (ICS-1100, Dionex, USA), respectively. The TDS concentration was obtained by calculating the mass concentrations of various ions.

To ensure the accuracy of the test results, the charge balance error (%CBE) (Ghahremanzadeh et al. 2018; Kumar et al. 2018; Adimalla and Qian 2019) and the recovery rate (Singh et al. 2017a, b) for each sample were calculated. As a result, the charge balance errors for all samples were less than ± 5%, and the recovery rate was 80–120%.

In this study, the SPSS software package (IBM) was used for the statistical analysis of the water sample data.

The hydrochemical software package AquaChem (Waterloo Hydrogeologic) was used to plot the Piper trilinear diagram for hydrochemical type analysis. In addition, the hydrochemical characteristics of the groundwater were analyzed using ion correlation analysis.

Results and discussion

Hydrochemical characteristics

Ion composition characteristics

The statistics of the hydrochemical parameters for the 34 mine water samples are shown in Table 1. As the table shows, the pH of the mine water ranged from 7.10 to 7.90 with a mean of 7.55, indicating that the mine water was

Table 1 Descriptive statistics of the main hydrochemical parameters

No.	Longitude	Latitude	pH	EC	TH	TDS	Na^+	K^+	Ca^{2+}	Mg^{2+}	Cl^-	SO_4^{2-}	HCO_3^-
M1	111.199	39.952	7.8	2888.29	283.33	1588.56	437.8	0.52	90.96	13.64	548.33	198.41	286.92
M2	111.205	39.948	7.5	3145.87	380.37	1730.23	445.89	1.21	111.40	24.81	605.53	230.26	312.34
M3	111.210	39.946	7.5	2880.38	321.67	1584.21	424.61	1.51	71.54	34.73	589.75	149.42	314.16
M4	111.216	39.943	7.6	2764.51	285.92	1520.48	412.32	0.63	76.65	22.95	530.58	191.06	286.92
M5	111.217	39.939	7.7	2732.22	377.82	1502.72	370.31	0.83	98.12	32.25	552.27	159.22	290.55
M6	111.191	39.945	7.4	2389.53	344.62	1314.24	304.78	2.14	102.20	21.71	408.29	181.27	296.00
M7	111.198	39.942	7.3	2626.51	262.93	1444.58	381.84	1.55	82.79	13.64	441.82	181.27	343.22
M8	111.203	39.940	7.6	3080.31	283.39	1694.17	478.2	0.76	78.70	21.09	621.31	186.16	308.71
M9	111.209	39.936	7.4	2841.07	319.10	1562.59	417.8	0.59	90.96	22.33	575.94	188.61	266.95
M10	111.212	39.931	7.3	3103.33	316.55	1706.83	471.57	1.46	85.85	24.81	644.97	176.37	303.26
M11	111.220	39.928	7.4	2779.80	321.63	1528.89	401.33	2.56	113.45	9.30	562.13	173.92	268.76
M12	111.222	39.928	7.4	2785.55	293.58	1532.05	421.01	1.68	69.50	29.15	572.00	186.16	254.23
M13	111.229	39.931	7.1	2663.56	278.22	1464.96	390.64	0.46	91.98	11.78	508.88	142.07	319.61
M14	111.226	39.923	7.9	2663.91	344.63	1465.15	365.79	0.57	96.07	25.43	502.96	186.16	288.74
M15	111.228	39.917	7.6	2395.02	321.65	1317.26	329.42	2.81	94.03	21.09	499.02	124.93	248.79
M16	111.224	39.915	7.7	2741.62	334.41	1507.89	393.81	0.59	107.31	16.12	585.80	146.97	257.87
M17	111.183	39.931	7.8	1803.60	268.04	991.98	219.54	0.49	77.68	17.98	270.22	139.62	266.95
M18	111.181	39.925	7.9	2702.25	326.75	1486.24	382.71	1.45	105.27	15.50	550.30	127.38	305.08
M19	111.181	39.915	7.2	2417.85	298.67	1329.82	345.19	2.1	93.01	16.12	508.88	139.62	226.99
M20	111.189	39.917	7.4	3435.56	375.25	1889.56	523.06	2.21	114.47	21.71	775.15	208.21	246.97
M21	111.196	39.920	7.5	1684.75	293.57	926.61	179	1.34	90.96	16.12	207.10	159.22	274.21
M22	111.192	39.911	7.7	2919.69	326.75	1605.83	432.8	0.87	96.07	21.09	607.50	195.96	252.42
M23	111.189	39.909	7.8	3086.80	344.62	1697.74	465.49	0.45	104.25	20.47	686.40	195.96	225.18
M24	111.184	39.904	7.9	2799.65	326.75	1539.81	411.83	2.32	97.09	20.47	615.39	137.17	257.87
M25	111.193	39.907	7.1	2893.85	326.75	1591.62	426.55	1.34	101.18	17.98	607.50	171.47	266.95
M26	111.195	39.902	7.5	2709.73	288.47	1490.35	407.29	1.67	82.79	19.85	583.83	115.13	281.47
M27	111.204	39.900	7.9	2618.64	298.67	1440.25	382.12	1.87	87.90	19.22	548.33	117.58	285.11
M28	111.211	39.906	7.6	2568.91	275.68	1412.90	379.81	0.68	95.05	9.30	536.49	105.33	286.92
M29	111.195	39.895	7.3	3075.69	352.29	1691.63	444.1	0.93	97.09	26.67	577.91	249.85	296.00
M30	111.202	39.885	7.5	2937.07	308.90	1615.39	438.52	0.67	85.85	22.95	575.94	210.66	281.47
M31	111.196	39.886	7.9	3433.45	390.60	1888.40	523.03	1.34	113.45	26.05	812.63	193.51	219.73
M32	111.193	39.888	7.7	3058.84	336.95	1682.36	453.86	1.21	113.45	13.02	641.03	188.61	272.39
M33	111.189	39.884	7.6	2496.89	283.33	1373.29	353.16	2.12	86.87	16.12	453.65	142.07	321.42
M34	111.164	39.930	7.2	2487.45	219.52	1368.10	377.05	1.56	66.43	13.02	422.09	193.51	296.00
Min			7.1	1684.7	219.52	926.61	179	0.45	66.43	9.3	207.1	105.33	219.73
Max			7.9	3435.6	390.6	1889.56	523.06	2.81	114.47	34.73	812.63	249.85	343.22
Mean			7.55	2753.31	315.04	1514.31	399.77	1.31	93.25	19.95	550.88	170.39	279.71
Std			0.24	364.75	37.39	200.61	70.47	0.66	13.01	6.04	115.92	33.96	28.74
Permissible limits of China (2006), WHO (2017) for drinking			6.5–8.5	–	450	1000	200		–	–	250	250	–

All parameters are expressed in mg/L except pH and EC (μS/cm)

slightly alkaline. The EC of the mine water ranged from 1684.70 to 3435.60 μS/cm. The TH of all the samples was in the range of 219.52–390.6 mg/L with an average of 315.04 mg/L, corresponding to slightly hard or hard water based on the classification of Chinese Standards for Drinking Water Quality (Ministry of Health of the P. R. China 2006; Li et al. 2010). The TDS was in the range of 926.61–1889.56 mg/L with an average of 1514.31 mg/L, revealing that most of the water samples were brackish (WHO 2017). These results indicated that most of the water samples were not potable. The standard deviations of the TH and TDS values were 37.39 and 200.61 mg/L, respectively,

with a much greater spread in the TDS values indicating that the geohydrologic conditions had a greater influence on the TDS of mine water (Liu et al. 2019b).

The cation content in the mine water was ranked in the following order (from highest to lowest): $Na^+ > Ca^{2+} > Mg^{2+}$. The Na^+ mass concentration was in the range of 179.00–523.06 mg/L with an average of 399.77 mg/L, the Ca^{2+} mass concentration was in the range of 66.43–114.47 mg/L with an average of 93.25 mg/L, while the Mg^{2+} mass concentration was in the range of 9.3–34.73 mg/L with an average of 19.95 mg/L. The anion content in the mine water was ranked from highest to lowest as $Cl^- > HCO_3^- > SO_4^{2-}$. The Cl^- mass concentration was in the range of 207.10–812.63 mg/L with an average of 550.88 mg/L. The SO_4^{2-} mass concentration was in the range of 105.33–249.85 mg/L with an average of 710.39 mg/L. The HCO_3^- mass concentration was

in the range of 219.73–343.22 mg/L with an average of 279.71 mg/L. These results showed that all the mine water samples were dominated by Na^+ and Cl^- with high standard deviations and TDS, indicating that the renewal capacity of groundwater in the study area was weak, and the ability to receive freshwater supply was poor as well (Li et al. 2018; Liu et al. 2019b).

Hydrochemical type

The use of a Piper trilinear diagram is conducive to understanding the main ion composition and hydrochemical type of the groundwater (Singh et al. 2010, 2012). Here, the Piper trilinear diagram was plotted according to the content of the main ions from the mine water in the study area (Fig. 2). As the figure shows, all mine water samples were close to the Cl^- and SO_4^{2-} end member, and far away from the $CO_3^{2-} + HCO_3^-$ end members. The anions were mainly Cl^- and SO_4^{2-} (anion triangular chart at the lower right corner). In the cation triangular chart, the water samples were distributed close to the Na^+ end member and far away from the Ca^{2+} and Mg^{2+} end members. These ions were probably obtained from the weathering dissolution of the carbonate and evaporite (Tiwari et al. 2017). All the water samples were located in the left quadrant of the diamond shape (region I), indicating that the amount of alkali metals exceeded that of alkaline-earth metals, and that the strong acid exceeded the weak acid. Therefore, the main hydrochemical type of the mine water was Cl–Na in the study area.

Correlation between the chemical indicators

The ions in groundwater do not exist in isolation, as they interact with each other to some extent, and the correlation relationships between them can reflect the main sources of the ions (Zaidi et al. 2019). The correlation matrix of various chemical indicators in the mine water (Table 2) showed that remarkably positive correlations ($P > 0.01$) existed between
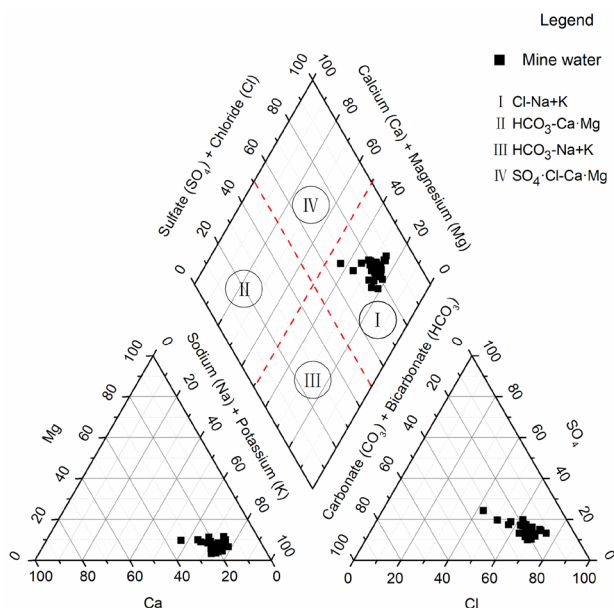
Fig. 2 Piper trilinear diagram of mine water

Table 2 Correlation matrix of the main hydrochemical parameters

	$Na^+ + K^+$	Ca^{2+}	Mg^{2+}	Cl^-	SO_4^{2-}	HCO_3^-	TH	TDS
$Na^+ + K^+$	1	0.263	0.252	0.943**	0.466**	−0.122	0.396*	0.983**
Ca^{2+}		1	−0.171	0.436**	0.161	−0.354	0.755**	0.380*
Mg^{2+}			1	0.3	0.309	−0.06	0.517**	0.323
Cl^-				1	0.298	−0.337	0.578**	0.948**
SO_4^{2-}					1	−0.008	0.345*	0.525**
HCO_3^-						1	−0.348	−0.12
TH							1	0.545**
TDS								1

*Correlation is significant at the 0.05 level (two tailed)

**Correlation is significant at the 0.01 level (two tailed)

TDS and Na^+, Ca^{2+}, Cl^-, and SO_4^{2-}, indicating that these ions contributed to TDS. In particular, the correlations between TDS with Na^+ and Cl^- were > 0.9, indicating that these two ions were the main sources of TDS. However, there were no obvious correlations between TDS and Mg^{2+} and HCO_3^-, and between Ca^{2+} and SO_4^{2-}, indicating that some chemical reactions might take place. For example, cation exchange, precipitation and crystallization can disturb the ion contents, which caused a weak correlation between TDS and Mg^{2+} as well as HCO_3^- (Li et al. 2018). In addition, Na^+ and Cl^- significantly correlated ($r = 0.943$), and their concentrations were both high, indicating that these ions were most likely derived from the dissolution of a single substance such as halite, whereas HCO_3^- was insignificantly correlated with Ca^{2+} and Mg^{2+}, suggesting that the dissolution of limestone does not play a significant role.

Analysis of influencing factors

Water–rock interaction

During the runoff process, the water continuously reacts with the surrounding rock minerals and is also influenced by atmospheric precipitation and evaporation condensation (Utom et al. 2013). Studying these influencing mechanisms therefore sheds light on the hydrochemical origins of groundwater. Gibbs (1944) first proposed the use of correlations between TDS and Na^+, Ca^{2+}, Cl^-, and HCO_3^- to study the formation mechanisms of the river surface water, including evaporative crystallization, rock weathering, and atmospheric precipitation effects. In recent years, the Gibbs map has been widely used to investigate the formation mechanism of groundwater (Tiwari et al. 2017; Liu et al. 2020).

Here, a Gibbs map was used to analyze all the mine water samples (Fig. 3). The results showed that the TDS values of the samples were relatively high (> 1000 mg/L), and that the
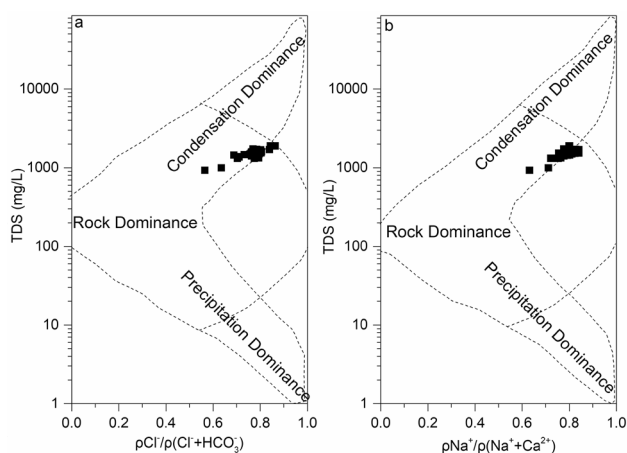
Fig. 3 Gibbs map of mine water in the study area

$Na^+/(Na^+ + Ca^{2+})$ ratios and $Cl^-/(Cl^- + HCO_3^-)$ ratios were from 0.6 to 0.8. The mine water samples therefore mainly occurred in the rock dominance area, indicating that the formation mechanism of the mine water in the study area was through water–rock interaction, whereas the contributions from evaporation and atmosphere precipitation were small.

Cation exchange

Cation exchange is another important process in the formation of groundwater hydrochemical components. Schoeller (1965) proposed the use of two indicators, CAI-1 and CAI-2, to determine the occurrence of cation exchange in the groundwater. The relevant equations are:

$$CAI - 1 = \frac{Cl^- - (Na^+ + K^+)}{Cl^-}, \tag{1}$$

$$CAI - 2 = \frac{Cl^- - (Na^+ + K^+)}{HCO_3^- + SO_4^{2-} + CO_3^{2-} + NO_3^-}. \tag{2}$$

If the two indicators are positive, it indicates that cation exchange has occurred as follows:

$$2Na^+ + (Ca, Mg)X_2 = (Ca, Mg)^{2+} + 2NaX. \tag{3}$$
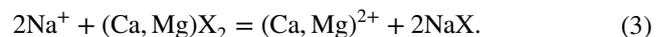
If, however, the two indicators are negative, it indicates the occurrence of reverse cation exchange as follows:

$$(Ca, Mg)^{2+} + 2NaX = 2Na^+ + (Ca, Mg)X_2. \tag{4}$$
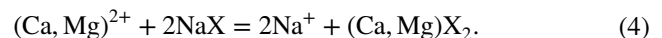
Figure 4a shows that both CAI-1 and CAI-2 were negative, indicating that reverse cation exchange occurred in the mine water. Further, the relationship between $(K^+ + Na^+ - Cl^-)$ and $(Ca^{2+} + Mg^{2+} - SO_4^{2-} - HCO_3^-)$ is also normally used to verify the presence of cation exchange in the groundwater, with a slope of around -1. In this case, the line of best fit between these quantities in the mine water samples was $Y = -0.9825X - 0.0183$ ($R^2 = 0.9962$) (Fig. 4b); hence, reverse cation exchange did occur in the study area.

Source analysis of main ions

The results presented thus far showed that the mine water in the study area was mainly controlled by rock mineral dissolution (Gan et al. 2018; Mahato et al. 2018). Figure 5 shows the relation diagram of Ca^{2+}/Na^+, HCO_3^-/Na^+, and Mg^{2+}/Na^+ of the evaporites, silicates and carbonates, whence it can be seen that the mine water samples were distributed between the silicates and evaporates, but were closer to the latter, indicating that the ion components in the mine water were mainly derived from the dissolution of evaporites. Through calculation of the saturation levels of the dolomite, calcite, gypsum, and halite (Fig. 6), it was found that
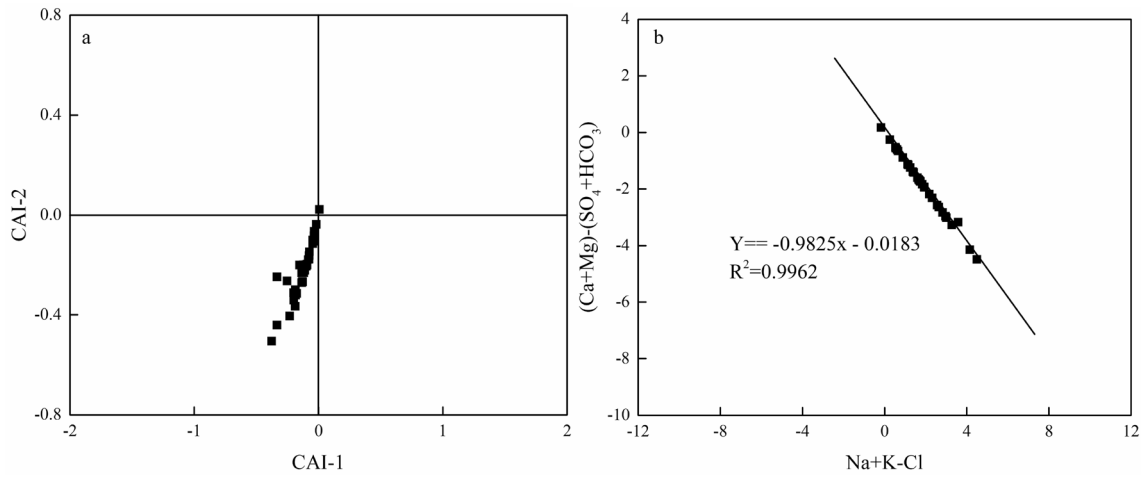
Fig. 4 Relationships between (**a**) CAI-1 and CAI-2 and (**b**) $(K^+ + Na^+ - Cl^-)$ and $(Ca^{2+} + Mg^{2+} - SO_4^{2-} - HCO_3^-)$
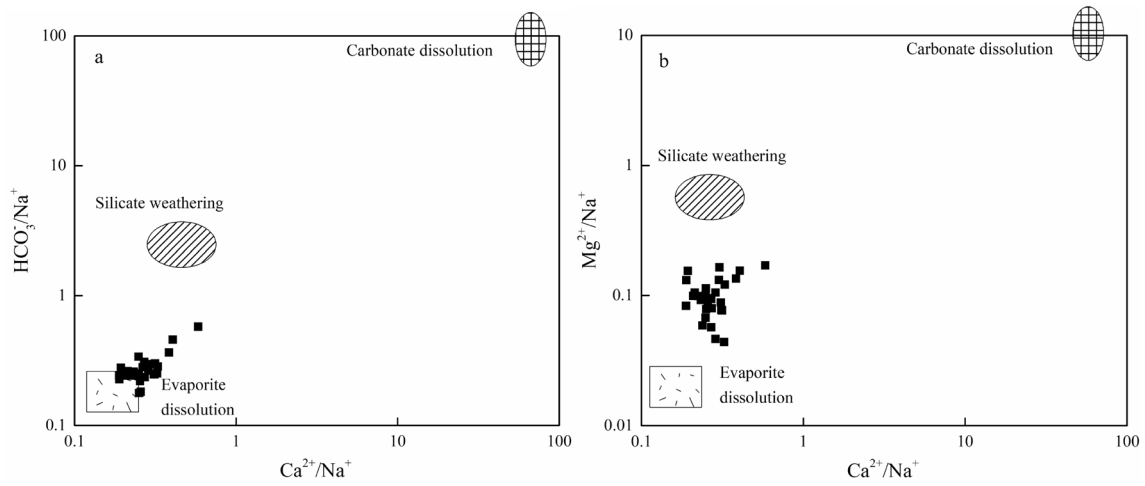
Fig. 5 Relationships between Ca^{2+} and Na^+, HCO_3^- and Na^+, and Mg^{2+} and Na^+
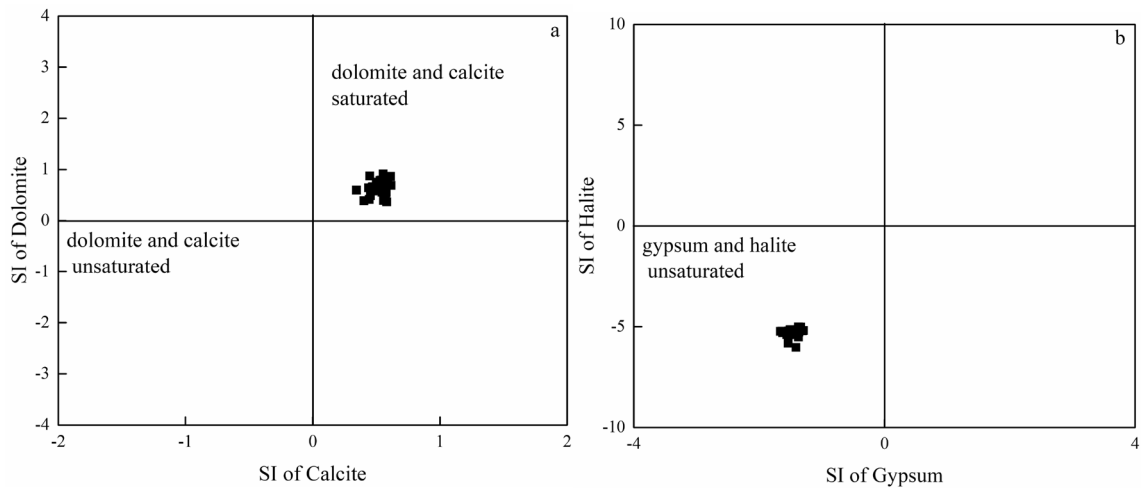
Fig. 6 Relationships between the saturation of: **a** dolomite and calcite, **b** gypsum and halite

the saturations of dolomite and calcite were both positive, while those of gypsum and halite were both negative. This indicated that the former two minerals were excessively dissolved and exhibited a saturated state with the occurrence of crystallization, whereas the latter two did not saturate and can therefore be further dissolved.

Additionally, the proportional relationships between the ions in the mine water (Fig. 7) can be used to determine their main sources (Li et al. 2018; Liu et al. 2019b). Figure 7a shows that the Na^+/Cl^- values of the mine water samples were close to one, further indicating that the dissolution of halite was the main source of the Na^+ and Cl^- in the mine water. The conclusion can be obtained that the dissolution of gypsum was the main source of SO_4^{2-} (Fig. 7b).

In the study area, the chemical composition of mine water was mainly controlled by water–rock interaction and the hydrochemical type was Cl–Na, which was mainly determined by regional hydrogeological conditions of karst groundwater. The Tangjiahui mining area is located in the residence area of the karst groundwater system in the Tianqiao spring area, with the original hydrochemical type bicarbonate. In the residence area, the groundwater flow rate was slower, residence time was longer and there was a greater time of contact between water and minerals. As the SI of carbonate minerals gradually increased, dolomite and calcite precipitated, and the groundwater was predominantly of the Cl–Na type, under the influence of cation exchange.

Suitability for human consumption

The mine water samples were compared with the drinking water standards recommended by the World Health Organization (WHO 2017) as well as by the Chinese government (Ministry of Health of the P. R. China 2006). Of the 34 samples, TDS was below 1000 mg/L in only 2, while all the others exceeded the quality limits for drinking water in China, making them unsuitable for human consumption without treatment (Table 1). The TH values of the analyzed water samples were within the slightly hard/hard range. The high TH, which is mainly due to Ca^{2+} and Mg^{2+}, may be
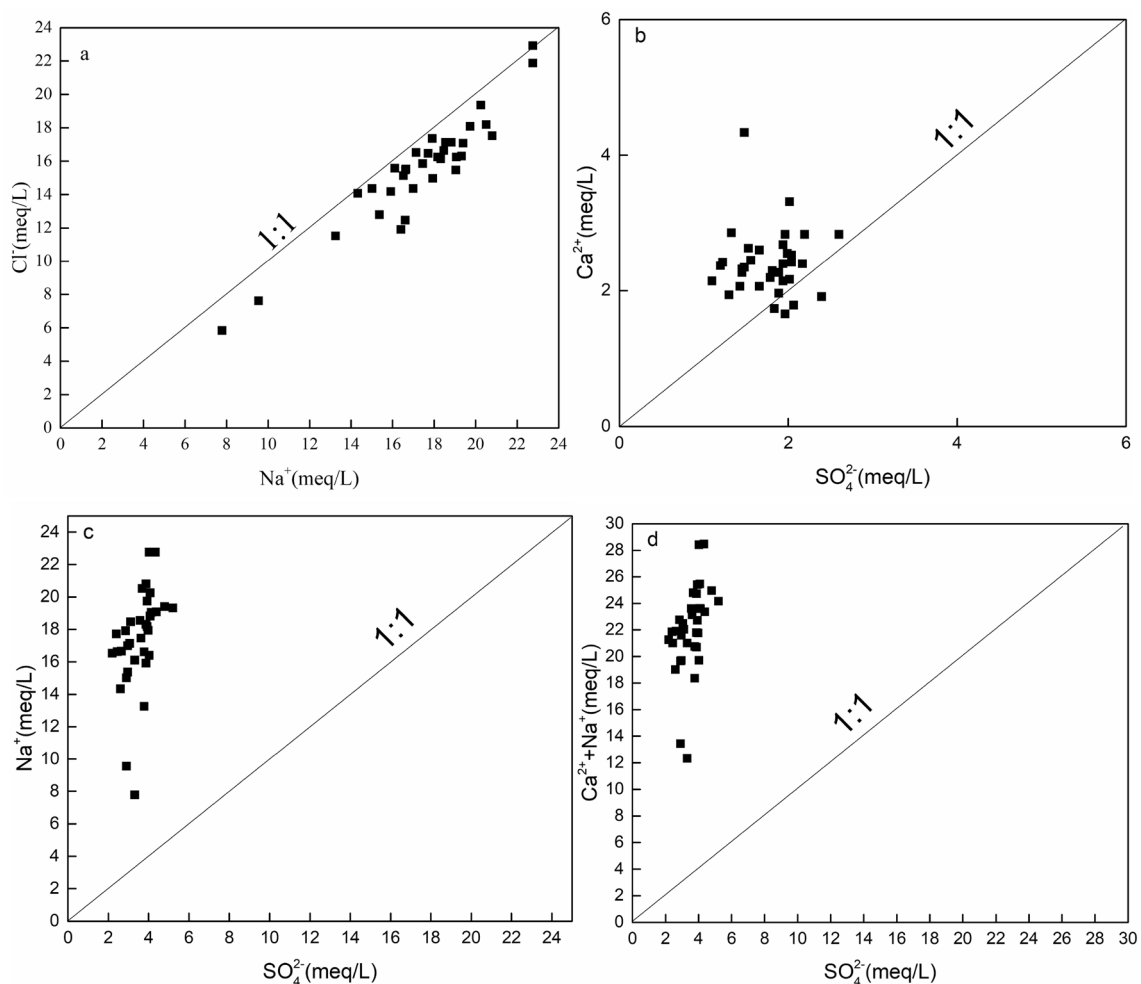
Fig. 7 The correlation between mine water ions in the study area: (**a**) $Na^+–Cl^-$, (**b**) $SO_4^{2-}–Ca^{2+}$, (**c**) $SO_4^{2-}–Na^+$, and (**d**) $SO_4^{2-}–(Ca^{2+}+Na^+)$.
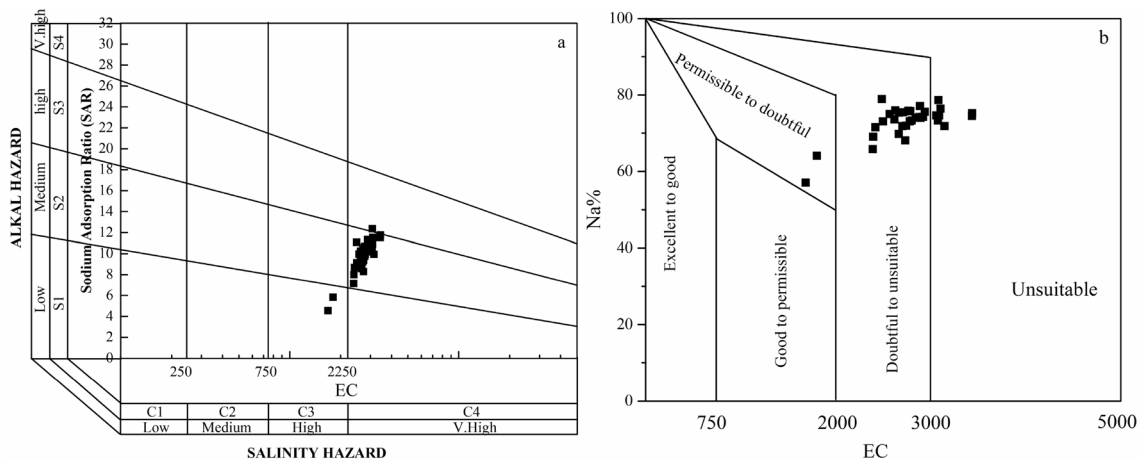
Fig. 8 USSL (**a**) and Wilcox (**b**) diagrams showing the suitability of the mine water for irrigation

attributed to the existence of alkaline soil. In addition, the concentration of $Na^+ + K^+$ and Cl^- in most mine water samples was above their acceptable limits (200 for $Na^+ + K^+$ and (250 mg/L for Cl^-) (Table 1). Therefore, mine water was not suitable for domestic consumption until it was treated.

Suitability for irrigation

Alkali and salinity hazard

The electrical conductivity (EC) and Na concentrations are of great importance in the classification of irrigation water (Ayers and Westcot 1985; Singh et al. 2010). Salts not only directly affect the growth of plants, but also affect the structure, permeability, and aeration of soil, which indirectly influence the growth of plants (Collins and Jenkins 1996). The total concentration of soluble salts in irrigation water can be classified as low (EC =< 250 $\mu S\ cm^{-1}$), medium (250~750 $\mu S\ cm^{-1}$), high (750–2250 $\mu S\ cm^{-1}$), and very high (2250–5000 $\mu S\ cm^{-1}$) (Richards 1954; Singh et al. 2010). The high EC leads to the formation of saline soil, while the high sodium concentration produces alkaline soil. In semi-arid regions, water losses through evaporation are a serious issue, as they often result in the presence of excess solute in irrigation water (Li et al. 2018; Liu et al. 2019a; Singh et al. 2010). These types of problems most commonly occur in areas with poor drainage, which causes the water level of groundwater to rise up to the vicinity of the plant rooting zone, leading to sodium salt accumulation by capillary ascent and evaporation (Mahato et al.2018; Singh et al. 2010).

The sodium adsorption ratio (SAR) or the alkali hazard is determined by both the absolute and relative concentration of the cations, which can be estimated using the following equation: $SAR = Na^+ / [(Ca^{2+} + Mg^{2+})/2]^{0.5}$. According to

the SAR value, the irrigation water can be classified into four levels (S1–S4): low (0–10), medium (10–18), high (18–26), and very high (> 26) (Richards 1954; Singh et al. 2010). The SAR of the mine water samples was in the range of 4.5 ~ 12.4. In the US salinity diagram (Fig. 8a), EC represents the salinity hazard and SAR represents the alkaline hazard. This indicated that most of the mine water samples were in the C4S2 region and the mine water was not suitable for irrigation.

Electrical conductivity (EC) and sodium percentage (Na%)

The sodium content (Na%) in the mine water samples was calculated according to the equation $Na\% = (Na^+ + K^+) / (Ca^{2+} + Mg^{2+} + Na^+ + K^+) \times 100$ (Wilcox 1955). The Na% values in the mine water samples were in the range of 57.1–78.9%. A high sodium content results in soil overturn and a decrease in permeability. The plot of EC vs. NA% (Fig. 8b) showed that most of the mine water samples were in the doubtful or unsuitable region, indicating that the water was not suitable for irrigation as well.

Conclusions

In this study, the hydrochemical characteristics analysis and quality assessment of mine water in Tangjiahui mining area, Inner Mongolia, China, were conducted. In addition, the main hydrochemical processes controlling the mine water chemistry were discussed. The main conclusions can be drawn as follows:

(1) The mine water in the study area was slightly alkaline and brackish water. The main cations and anions were

Na^+ and Cl^-, respectively, and the main hydrochemical type was Cl–Na.

(2) The water chemical composition in the study area was mainly derived from the dissolution of halite and gypsum, and reverse cation exchange in the mine water. The saturation of dolomite and calcite in the mine water was positive, while that of gypsum and halite was negative.

(3) Due to its high TDS, EC, SAR, and Na%, the mine water in the study area was not suitable for human consumption and agricultural irrigation.

The results of this study are significant to mine water resources management in the study area. Due to the poor quality, the mine water cannot be discharged at random and needs to be properly treated and reasonably managed by the government.

References

Adimalla N, Qian H (2019) Groundwater quality evaluation using water quality index (WQI) for drinking purposes and human health risk (HHR) assessment in an agricultural region of Nanganur, South India. Ecotoxicol Environ Safe 176:153–161

Ayers RS, Wascot DW (1985) Water quality for irrigation. FAO Irrigation and Drainage Paper #20, Rev 1, FAO, Rome

Cloutier V, Lefebvre R, Therrien R et al (2008) Multivariate statistical analysis of geochemical data as indicative of the hydrogeochemical evolution of groundwater in a sedimentary rock aquifer system. J Hydrol 353(3):294–313

Collins R, Jenkins A (1996) The impact of agricultural land use on stream chemistry in the middle hills of the Himalayas, Nepal. J Hydrol 185(1–4):71–86

EIA (2019) EIA projects that renewables will provide nearly half of world electricity by 2050[EB/OL]. https://www.eia.gov/today inenergy/detail.php?id=41533. Accessed 2 Oct

Gan YQ, Zhao K, Den g YM et al (2018) Groundwater flow and hydrogeochemical evolution in the Jianghan plain, central China. Hydrogeol J 26(11):1–15

Ghahremanzadeh H, Noori R, Baghvand A et al (2018) Evaluating the main sources of groundwater pollution in the southern Tehran aquifer using principal component factor analysis. Environ Geochem Health 40(4):1317–1328

Gibbs RJ (1970) Mechanisms controlling world water chemistry. Science 170(3962):1088–1090

Huang XJ, Wang GC, Liang XY et al (2017) Hydrochemical and Stable Isotope (δD and δ^{18}O) Characteristics of Groundwater and hydrogeochemical processes in the Ningtiaota coalfield Northwest China. Mine Water Environ 37(1):119–136

Kumar S, Venkatesh AS, Singh R et al (2018) Geochemical signatures and isotopic systematics constraining dynamics of

fluoride contamination in groundwater across Jamui district, Indo-Gangetic alluvial plains, India. Chemosphere 205:493–505

Li P (2018) Mine water problems and solutions in china. Mine Water Environ 37(2):1–5

Li P, Qian H, Wu J (2010) Groundwater quality assessment based on improved water quality index in Pengyang County, Ningxia, northwest China. J Chem 7(S1):S209–S216

Li P, Qian H, Wu J et al (2013a) Major ion chemistry of shallow groundwater in the Dongsheng Coalfield, Ordos Basin, China. Mine Water Environ 32(3):195–206

Li P, Wu J, Hui Q (2013b) Assessment of groundwater quality for irrigation purposes and identification of hydrogeochemical evolution mechanisms in Pengyang County China. Environ Earth Sci 69(7):2211–2225

Li P, Qian H, Howard KWF, Wu J (2015) Building a new and sustainable '"Silk Road economic belt."' Environ Earth Sci 74(10):7267–7270

Li P, Tian R, Liu R (2018) Solute geochemistry and multivariate analysis of water quality in the Guohua phosphorite mine, Guizhou Province, China. Expo Health 11(2):81–94

Li QL, Kong WJ, Liu WW (2020) Ordovician lime water prevention and control technology in fully mechanized top-coal caving face of Tangjiahui Coal Mine. Coal Eng 52(S0):92–95 (**in Chinese**)

Liu J, Gao M, Wang T et al (2019a) Hydrochemical processes and groundwater quality assessment in Yushenfu mining area, Northwest China. Desalin Water Treat 165:177–187

Liu J, Jin D, Wang T et al (2019b) Hydrogeochemical processes and quality assessment of shallow groundwater in Chenqi coalfield, Inner Mongolia, China. Environ Earth Sci 8(12):347

Liu J, Wang H, Jin D et al (2020) Hydrochemical characteristics and evolution processes of karst groundwater in Carboniferous Taiyuan formation in the Pingdingshan coalfield. Environ Earth Sci 79(6):151

Mahato MK, Singh P, Singh AK, Tiwari AK (2018) Assessment of hydrogeochemical processes and mine water suitability for domestic, irrigation, and industrial purposes in east Bokaro Coalfield India. Mine Water Environ 37(3):493–504

Ministry of Health of the P. R. China, Standardization Administration of the P. R. China (2006) Standards for drinking water quality (GB 5749–2006). China Standard Press, Beijing (**in Chinese**)

Piper AM (1944) A graphical procedure in the geochemical interpretation of water analysis. Am Geophys Union Trans 25:914–928

Redwan M, Abdel Moneim AA, Amra MA (2016) Effect of water-rock interaction processes on the hydrogeochemistry of groundwater west of Sohag area. Egypt Arab J Geosci 9(2):111

Richards LA (1954) Diagnosis and improvement of saline and alkali soils, US Dept Agriculture Handbook #60, Washington DC, USA: 166

Schneider L, Maher WA, Rose NL et al (2020) Assessing environmental contamination from metal emission and relevant regulations in major areas of coal mining and electricity generation in Australia. Sci Total Environ 728:137398

Schoeller H (1965) Qualitative evaluation of groundwater resources. In: Methods and techniques of groundwater investigation and development. Water Research, Series-33. UNESCO, Delft: 54–83.

Sefie A, Aris AZ, Ramli MF et al (2018) Hydrogeochemistry and groundwater quality assessment of the multilayered aquifer in Lower Kelantan Basin, Kelantan Malaysia. Environ Earth Sci 77(10):397

Singh AK, Mahato MK, Neogi B et al (2010) Quality assessment of mine water in the Raniganj Coalfield Area, India. Mine Water Environ 29(4):248–262

Singh AK, Mahato MK, Neogi B et al (2012) Environmental geochemistry and quality assessment of mine water of Jharia coalfield, India. Environ Earth Sci 65(1):49–65

Singh R, Syed TH, Kumar S et al (2017a) Hydrogeochemical assessment of surface and groundwater resources of Korba coalfield, Central India: environmental implications. Arab J Geosci 10(14):318

Singh R, Venkatesh AS, Syed TH et al (2017b) Assessment of potentially toxic trace elements contamination in groundwater resources of the coal mining area of the Korba Coalfield, Central India. Environ Earth Sci 76(16):566

Tiwari AK, Singh AK, Singh MP (2017) Hydrogeochemical analysis and evaluation of surface water quality of Pratapgarh district, Uttar Pradesh, India. Appl Water Sci 7(4):1609–1623

Utom AU, Odoh BI, Egboka BCE (2013) Assessment of hydrogeochemical characteristics of groundwater quality in the vicinity of Okpara coal and Obwetti fireclay mines, near Enugu town, Nigeria. Appl Water Sci 3(1):271–283

Wang L, Dong Y, Xu Z et al (2017) Hydrochemical and isotopic characteristics of groundwater in the northeastern Tennger Desert, northern China. Hydrogeol J 25(8):2363

WHO (2017) Guidelines for drinking-water quality: fourth edition incorporating the first addendum. World Health Organization, Geneva, p 631

Wilcox LV (1955) Classification and use of irrigation waters, vol. 969. USDA Circular, Washington DC: 19

Wu Q, Shen JJ, Wang Y (2017) Mining techniques and engineering application for "Coal-Water" dual-resources mine. J China Coal Soc 42(1):8–16

Xu J, Chen M, Hong H et al (2019) Differences of hydraulic conductivities from Pumping and draining tests with intensity effects. J Hydrol 579:124165

Yu Y, Yang JF, Yang ZX et al (2020) Global mining market in 2019: overview and outlook. China Min Mag 29(2):1–5 (**in Chinese**)

Zaidi FK, Salman A, Hag-Elsafi S et al (2019) Assessment of hydrological processes operating in a multi-layered sedimentary aquifer system in Saudi Arabia using integrated chemical and statistical approach. Environ Monit Assess 191(7):460